Inorganica Chimica Acta 429 (2015) 15–21

Contents lists available at ScienceDirect

Inorganica Chimica Acta

journal homepage: www.elsevier.com/locate/ica

Nitrito complexes of nickel(II), copper(II) and cobalt(II) with tridentate pyrazole based planer ligand: Structure, spectroscopy, thermal properties and imitative nuclease activity

Cigdem Hopa [a,*], Raif Kurtaran [b], Ersin Hopa [c], Gulcin Cetin [d], Ekrem Dundar [e], Hulya Kara [f], Mahir Alkan [a]

[a] University of Balikesir, Faculty of Science and Literature, Department of Chemistry, 10145 Balikesir, Turkey
[b] Akdeniz University, Alanya Engineering Faculty, Materials Science and Engineering, 07425 Alanya, Antalya, Turkey
[c] Pamukcu Multi-Program High School, Balikesir, Turkey
[d] Bilecik Seyh Edebali University, Faculty of Science and Literature, Department of Molecular Biology and Genetics, 11210 Bilecik, Turkey
[e] University of Balikesir, Faculty of Science and Literature, Department of Biology, 10145 Balikesir, Turkey
[f] University of Balikesir, Faculty of Science and Literature, Department of Physics, 10145 Balikesir, Turkey

ARTICLE INFO

Article history:
Received 20 November 2014
Accepted 16 December 2014
Available online 7 February 2015

Keywords:
2,6-Bis(3,4,5-trimethyl-N-pyrazolyl)pyridine
Nitrito complexes
X-ray structure
DNA interaction

ABSTRACT

Functional documentation of metal complexes are essential for various aspects including gene function/regulation and drug design for lethal diseases like cancer (Sigel and Martin (1982), Peters et al. (1997), Martin and Mascharak (2000), Hazra et al. (2007), Zhang et al. (2002), Patra et al. (2003)). Therefore, we have synthesized three new nitrite bound coordination complexes with the ligand 2,6-bis (3,4,5-trimethylpyrazole)pyridine (btmpp), [Ni(btmpp)(ONO)$_2$] (**1**), [Cu(btmpp)(ONO)$_2$] (**2**) and [Co(btmpp)(ONO)$_2$] (**3**) and complexes were characterized by elemental analysis, IR spectroscopy and X-ray single-crystal diffraction analysis. Thermal stabilities of these complexes were studied by thermogravimetric (TG) and differential thermal analyses (DTA). The single crystal X-ray analyses showed that the geometry around the Ni atom was distorted octahedral with NiN_3O_3 coordination sphere. One of the nitrites in complex **1** is terminally bonded to the metal centre through the oxygen atom, whereas the other one is chelated as a bidentate through both oxygen atoms. In complex **2**, the coordination around the Cu atom is a distorted square-pyramid ($\tau = 0.083$) involving three N atoms from btmpp and two oxygen atoms from nitrites. Both nitrite groups are terminally bonded to the metal. DNA interaction properties of the compounds were also analyzed by agarose gel electrophoresis. The results indicated that all of the complexes converted supercoiled plasmid DNA (pET21a) into its nicked-circular form without addition of any external agents at physiological conditions. Complex **2** was the most effective on the cleavage of DNA, and its activity was observed as a conversion of double stranded DNA into nicked and linear form.

1. Introduction

Investigations on the interaction between transition metal complexes containing multidentate aromatic ligands, and DNA has gained much attention due to their varied applications including the design and development of artificial nucleases, potential uses of new chemotherapeutic agents, gen regulators and spectroscopic probes of DNA [1–6]. Among the transition metal complexes, complexes of copper(II) ion due to their labile coordination sphere, are preferred molecules for their DNA cleavage potentials. This is because of the fact that these complexes can not only bring about oxidative cleavage of DNA, but also they can perform hydrolytic, photolytic and electrolytic cleavage of DNA [7,8]. Studies comparing the transition metal complexes reported that copper(II) complexes and zinc(II) complexes can cleave DNA in the absence of any added redox agents but nickel(II) and cadmium(II) complexes are reported to present relatively less activity [9].

Coordination chemistry of NO_2^- including complexes are also attractive due to their importance in biosystems. Interaction of NO_2^- with several hemoproteins is known [10]. The nitrite ion is known to coordinate the metal ions in various ways. It's well known that the ambidentate NO_2^- ligand can be coordinated either to oxygen or to nitrogen in monodentate metal complexes while nitrito complexes are less common [11]. It may also act as a chelating ligand (via both oxygen atoms) to yield mononuclear complexes. The first example of chelating nitrite group was synthesised by Goodgame [12] in some Co(II) and Ni(II) nitrite complexes.

* Corresponding author. Tel.: +90 266 6121000; fax: +90 266 6121215.
E-mail addresses: cigdem@balikesir.edu.tr, cigdemhopa@gmail.com (C. Hopa).

http://dx.doi.org/10.1016/j.ica.2014.12.035
0020-1693/

Moreover, five bridging modes of nitrite ions have been identified in polynuclear complexes. Binding modes of nitrite ions are shown in Scheme 1. The two atom O–N bridging mode is the most common one, and it usually shows mild antiferromagnetic interactions.

Although biological importance of nitrite including complexes and pyrazole derivative 2,6-bis(pyrazole)pyridine (pp) ligand family are very common in coordination chemistry, there isn't any report about nitrito complexes with btmpp to date, which prompted us to synthesize some nitrito complexes with btmpp. Also to our knowledge, only a few articles about the interaction of DNA with metal-pp ligand complexes are reported. Very recently Cu(II) and Ni(II) complexes have been reported to be active in DNA strand cleavage [13,9]. Also, different complexes synthesized from same ligands with different metal ions may exhibit different biological properties. In this respect, synthesis of novel compounds having different biological activities is very important. The newly synthesized complexes may be more effective than known others in terms of their biological applications [14].

Hence, in continuation with our earlier work on pp ligand family [15], here we report the synthesis, crystal structure, spectroscopic, thermal characterisation and DNA cleavage property of Cu(II), Ni(II) and Co(II) nitrito complexes with pyrazole based btmpp ligand (Scheme 2).

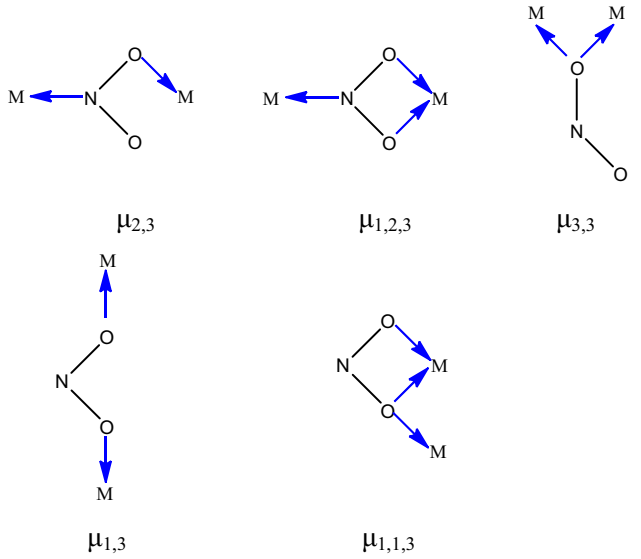

Scheme 1. The binding modes of nitrate molecule to metal ion. M = metal.

2. Experimental

2.1. Material and measurements

All chemicals were purchased from Merck (Darmstadt, Germany) and Aldrich (Steinheim, Germany) and used without further purifications. The elemental analysis for the ligands and complexes were carried out at the Eurovector 3018 CHNS analyzer. Melting points were obtained using a STUART Melting Point SMP3. The IR spectra were obtained by using IR grade KBr disks on a Perkin-Elmer 1600 Series FTIR spectrophotometer in the range of 4000–400 cm^{-1}. The electronic spectra were recorded in a Cary 1E UV–Vis spectrophotometer (Varian, Darmstadt, Germany). Thermal behaviour of the complexes was performed with a Perkin Elmer Diamond DTA/TG thermal analyzer at a heating rate of 20 °C/min in nitrogen (3 bar) with a flow rate of 200 mL/min in ceramic crucibles.

2.2. Preparation of the ligand

Btmpp was easily prepared in one step by the reaction of 2,6-dichloropyridine and sodium salt of 3,4,5-trimethylpyrazole in diglyme as described previously [16].

2.3. Preparation of complexes **1–3**

All three compounds were synthesized by a following similar method. A solution of metal salt (1 mmol) in EtOH or MeOH (20 mL) was added into the stirred solution of btmpp in EtOH (20 mL). To this solution, freshly-prepared $NaNO_2$ (2 mmol) in an aqueous solution (5 mL) was added with constant stirring. Resulting reaction mixtures were then filtered to remove any impurity and left to evaporate in room temperature. After a few days, the

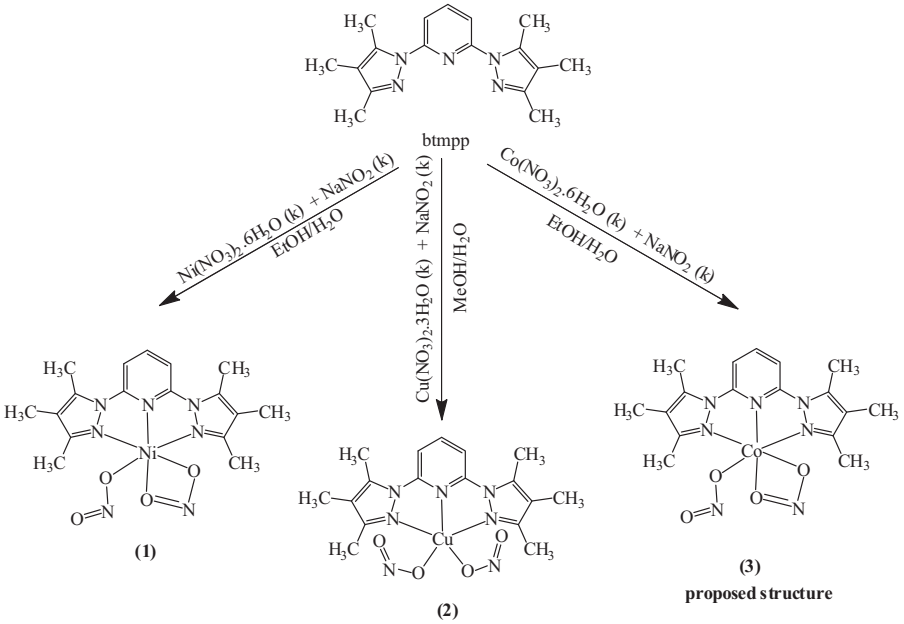

Scheme 2. Synthetic pathway for complexes **1–3**.

Table 1
Crystal data and structure refinements for **1** and **2**.

	1	**2**
Chemical formula	$NiC_{17}H_{21}N_7O_4$	$CuC_{17}H_{21}N_7O_4$
M_w	446.10	450.94
Crystal system	monoclinic	monoclinic
Space group	$P2_1/c$	$P2_1/n$
Unit cell dimensions		
a (Å)	8.2408(4)	8.2444(2)
b (Å)	18.8074(7)	12.8380(2)
c (Å)	12.7642(5)	19.4042(5)
α (°)	90	90
β (°)	94.064(3)	100.3840(10)
γ (°)	90	90
V (Å^3)	1973.3(1)	2020.13(8)
T (K)	293(2)	293 (2)
Z	4	4
ρ_{calc} (g cm^{-3})	1.501	1.466
μ (mm^{-1})	1.023	1.483
Reflections collected	70618	76836
Independent reflections	3439	3794
Goodness-of-fit (GOF) on F^2	1.115	0.958
R indices [$I > 2\sigma(I)$]	$R_1 = 0.05$, $wR_2 = 0.12$	$R_1 = 0.10$, $wR_2 = 0.13$

resulting crystals were filtered and dried (Scheme 2). *Anal.* Calc. for $C_{17}H_{21}N_7O_4Ni$: C, 45.8; H, 4.7; N, 22.0. Found: C, 46.4; H, 4.6; N, 21.9%. UV–Vis [λ_{max}, nm ε (M^{-1} cm^{-1})] in DMF: 264.2 (16300); 274.3 (19300); 306.5 (10700); 333.6 (12900); 607.8 (14). *Anal.* Calc. for $C_{17}H_{21}CuN_7O_4$: C, 45.3; H, 4.7; N, 21.1. Found: C, 43.5; H, 4.9; N, 20.9%. UV–Vis [λ_{max}, nm ε (M^{-1} cm^{-1})] in DMF: 260.2 (18700); 266.3 (18800); 304.3 (18800); 682.1 (105). *Anal.* Calc. for $C_{17}H_{21}CoN_7O_4$: C, 45.8; H, 4.7; N, 22.0. Found: C, 46.7; H, 4.7; N, 22.6%. UV–Vis [λ_{max}, nm ε (M^{-1} cm^{-1})] in DMF: 257.4 (13100); 265.3 (16300); 304.6 (16100); 535.0 (51).

2.4. X-ray crystallography

All measurements were made on a Rigaku R-AXIS RAPID-S imaging plate area detector with graphite monochromated Mo Kα (λ = 0.71070 Å) radiation and were corrected for Lorentz and polarization effects. The structure was solved by direct methods [17] and expanded using Fourier techniques [18]. The non-hydrogen atoms were refined anisotropically. Hydrogen atoms were refined isotropically by full-matrix least-squares. All calculations were performed using the Crystal Structure [19,20] crystallographic software package. Crystal data collection conditions and parameters of refinement process of the complexes **1** and **2** are summarized in Table 1. Displacement ellipsoids shown in Figs. 1 and 2 are plotted at the 40% probability level.

2.5. DNA cleavage studies

The DNA cleavage analysis was carried out on a 12 μL total sample volume in 0.2 mL Eppendorf tubes containing pET21a plasmid DNA (Novagen) (200 ng), and the results were visualized through agarose gel electrophoresis. For the DNA cleavage analysis, pET21a plasmid DNA (Novagen, USA) was treated with different concentrations of the ligand and complexes (200–1000 μM). The reactions were incubated in the dark for 3 h at 37 °C and then a 2 μL of 6X DNA loading dye (Thermo Scientific, USA), were added to 10 μL of the metal complex-DNA solution. The samples were loaded onto a 0.8% agarose gel with 1X TAE buffer (40 mM Tris, 20 mM Acetic acid and 1 mM EDTA), the gel was then stained with ethidium bromide at a concentration of 1 μg/mL. The gel was run at 96 V for 1 h, visualized by a gel documentation system (Vilber Lourmat, Germany) and photographed. Quantification of DNA bands were also performed using the software of the same gel documentation system.

3. Results and discussion

3.1. IR spectra

IR assignments of the most important vibrational bands for free btmpp, free nitrite and the complexes **1**–**3** are shown in Table 2. The IR spectra for all three complexes were similar, implying that they were structurally alike. And the bands observed in the IR spectrum of the free btmpp ligand at 1599 and 1583 cm^{-1}, showing a non-coordinated pyridine ring, were shifted to higher frequencies upon complexation with metal centre.

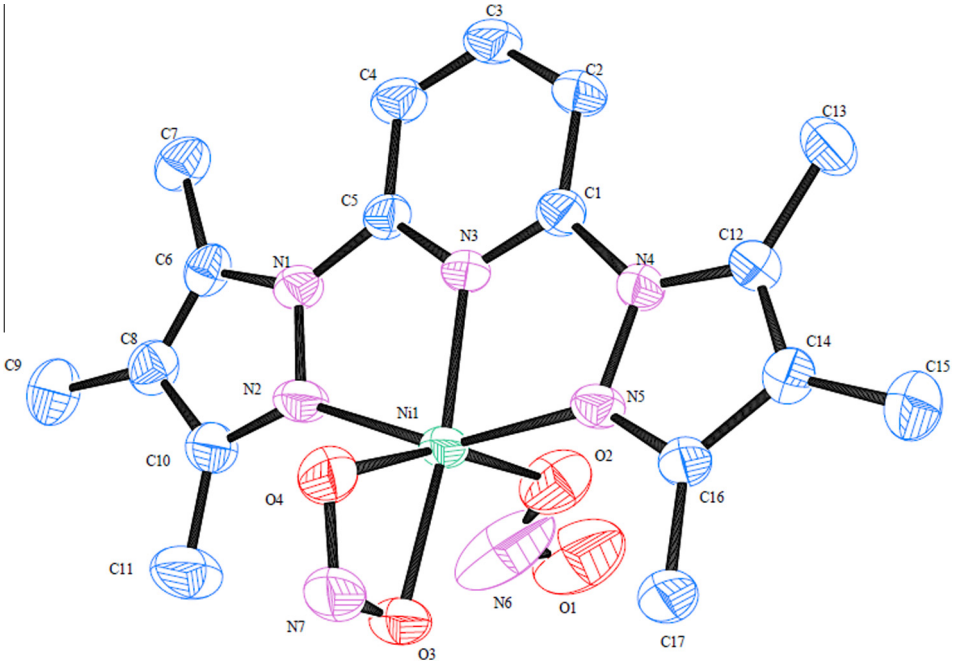

Fig. 1. Ortep plot of complex **1**. The thermal ellipsoid for the image represents a 40% probability limit.

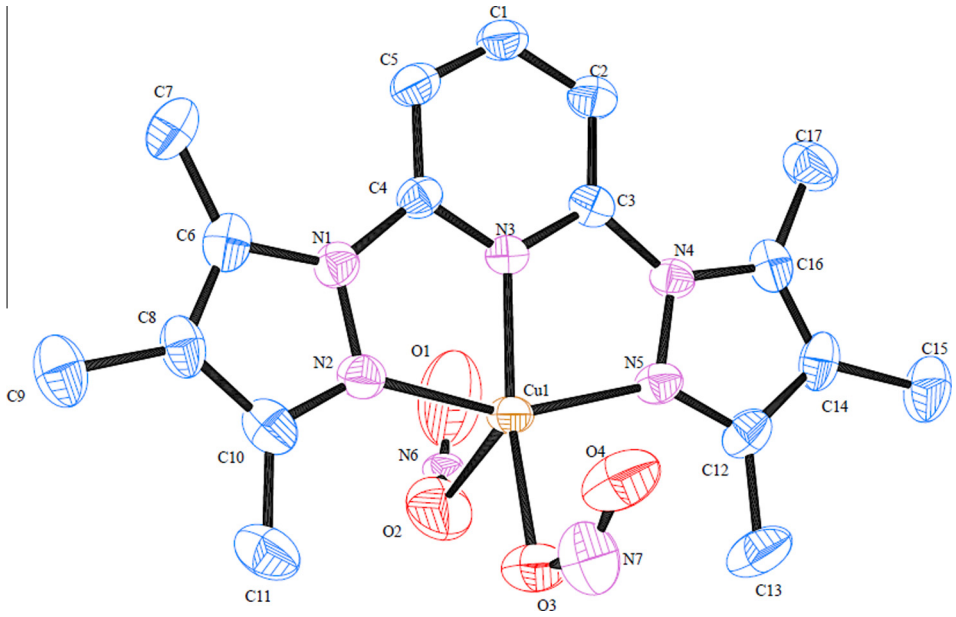

Fig. 2. Ortep plot of complex **2**. The thermal ellipsoid for the image represents a 40% probability limit.

Table 2
IR assignments of the most important vibrational bands for free btmpp, free nitrite and the complexes.

	$\nu_{as}(NO_2)$ (cm^{-1})	$\nu_s(NO_2)$ (cm^{-1})	$\nu_b(NO_2)$ (cm^{-1})
Free nitrite ($NaNO_2$) [21]	1328	1261	828
Chelating nitrite [22]	1266–1390	1171–1225	840–866
Complex **1**	1319	1209, 1013	844
Complex **2**	1325	1034	848
Complex **3**	1317	1205, 1022	844

Table 3
Some selected bond lengths [Å] and angles [°] for **1** and **2**.

	1	**2**	
Bond distances (Å)			
Ni(1)–N(2)	2.077(4)	Cu(1)–N(2)	2.033(4)
Ni(1)–N(3)	2.018(4)	Cu(1)–N(3)	1.971(4)
Ni(1)–N(5)	2.082(4)	Cu(1)–N(5)	2.021(4)
Ni(1)–O(2)	2.053(5)	Cu(1)–O(2)	2.19(2)
Ni(1)–O(3)	2.068(4)	Cu(1)–O(3)	2.005(6)
Ni(1)–O(4)	2.170(4)		
Bond angles (°)			
N(3)–Ni(1)–N(2)	76.8(1)	N(3)–Cu(1)–N(2)	78.3(2)
N(3)–Ni(1)–N(5)	76.9(1)	N(3)–Cu(1)–N(5)	78.0(2)
N(5)–Ni(1)–N(2)	152.9(2)	N(5)–Cu(1)–N(2)	155.2(2)
N(3)–Ni(1)–O(2)	91.1(2)	N(3)–Cu(1)–O(2)	117.7(4)
N(3)–Ni(1)–O(3)	166.9(2)	N(3)–Cu(1)–O(3)	160.2(2)
N(5)–Ni(1)–O(2)	87.8(2)	N(5)–Cu(1)–O(2)	102.7(3)
O(2)–Ni(1)–N(2)	98.9(2)	N(5)–Cu(1)–O(3)	100.7(2)
O(3)–Ni(1)–O(2)	101.8(2)	O(3)–Cu(1)–N(2)	99.1(2)
O(3)–Ni(1)–O(4)	58.8(2)	O(2)–Cu(1)–N(2)	94.6(3)
O(3)–Ni(1)–N(2)	103.1(1)	O(2)–Cu(1)–O(3)	82.0(4)
O(3)–Ni(1)–N(5)	101.1(1)		
O(4)–Ni(1)–N(2)	91.5(2)		
O(4)–Ni(1)–N(3)	108.1(1)		
O(4)–Ni(1)–N(5)	90.7(1)		
O(4)–Ni(1)–O(2)	159.9(2)		

The nitrite group (C_{2v}) had three fundamental vibrational modes which were all IR active in the IR region. Upon coordination number of IR active frequencies did not change but the band positions were shifted as compared to the free nitrite frequencies. The shifts exhibited by the asymmetric and symmetric stretching frequencies were used to interpret the binding mode of the nitrite group. In nitro complexes, both $\nu_s(NO_2)$ and $\nu_{as}(NO_2)$ were shifted to higher frequencies. However, nitrito complexes, $\nu_{as}(NO_2)$ lied at higher and $\nu_s(NO_2)$ at lower values as compared to the free nitrite ion [23]. If the nitrito group is chelating, the asymmetric and symmetric $\nu(NO_2)$ of the nitrito group will be shifted to a lower frequency. Because this type of chelate formation reduces two N–O bonding degrees [24]. Furthermore all nitro complexes had several sharp bands of medium intensity between 630 and 560 cm^{-1} but in nitrito complexes there weren't such bands near 600 cm^{-1} [25]. According to the results obtained from IR spectra of complexes **1**–**3**, the absence of the characteristic bands of the nitro complex near 600 cm^{-1} also suggests that the NO_2 group is linked to the metal centres through an oxygen atom. In complex **1**, the bands at 1319; 1209, 1013 and 844 cm^{-1} were tentatively assigned to $\nu_{as}(NO_2)$, $\nu_s(NO_2)$ and $\nu_b(NO_2)$ respectively and these stretches were shifted to lower frequency and $\nu_b(NO_2)$ frequency was shifted to upper frequency compared to free NO_2 group. Therefore it is mentioned that the existence of chelate formed the nitrite group in the structure via the two O atoms. The same bands were observed at 1317; 1205, 1022 and 844 cm^{-1} for **3**. There weren't any bands between 1200 and 1220 cm^{-1} in complex **2** which indicated the terminally connected O-coordinated nitrite. This is good agreement with the structure of **2** solved by X-ray technique.

3.2. Electronic spectra

The electronic spectra of complexes **1**–**3** and the btmpp ligand were recorded in DMF, because the complexes are sufficiently soluble in this solvent only. All three complexes displayed strong absorption bands between 257 and 333 nm (for complex **1**; 264.2 nm (16300 M^{-1} cm^{-1}), 274.3 nm (19300 M^{-1} cm^{-1}), 306.5 nm (10700 M^{-1} cm^{-1}) and 333.6 nm (12900 M^{-1} cm^{-1}), for complex **2**; 260.2 nm (18700 M^{-1} cm^{-1}), 266.3 (18800 M^{-1} cm^{-1}) and 304.3 nm (18800 M^{-1} cm^{-1}), for complex **3**; 257.4 nm (13100 M^{-1} cm^{-1}), 265.3 nm (16300 M^{-1} cm^{-1}) and 304.6 nm (16100 M^{-1} cm^{-1})). These are clearly charge transfer origin and

assigned to intraligand π–π* transitions in the complexes [26]. Very weak, low-intensity absorption bands at 607.8 nm (14 M^{-1} cm^{-1}) for **1**, 682.1 nm (105 M^{-1} cm^{-1}) for **2** and 535 nm (51 M^{-1} cm^{-1}) for **3** were associated with d–d transition of the metal atoms.

3.3. Structural analysis of *1* and *2*

The molecular structures consists of neutral [Ni(btmpp)$(ONO)_2$] molecule for **1** and [Cu(btmpp)$(ONO)_2$] molecule for **2**, respectively. The geometry around the nickel(II) in complex **1** was best described as a distorted octahedron with NiN_3O_3 chromophore. Three nitrogen atoms (N2, N3, N5) of the btmpp ligand and an oxygen atom (O3) from chelating nitrite molecule defined the equatorial plane around the nickel atom. The apical positions of the octahedron were occupied by an oxygen atom (O2) of terminally bonded nitrite molecule and an oxygen atom (O4) of chelating nitrite molecule. The axial bond distances were Ni(1)–O(2) = 2.053(5) and Ni(1)–O(4) = 2.170(4) Å, and the equatorial bond distances were Ni(1)–N(2) = 2.077(4), Ni(1)–N(3) = 2.018(4), Ni(1)–N(5) = 2.082(4) and Ni(1)–O(3) = 2.068(4) Å. The nitrite ion can coordinate to Ni(II) atom in a variety of modes, with both *N*-(nitro) coordination, or more commonly with *O*-(nitrito) coordination, which can be unidentate, symmetrical or unsymmetrical chelate, or as a variety of a bridging modes. As a result of unsymmetrical chelating mode, Ni(1)–O(3) bond distance (2.068(4)) was shorter than Ni(1)–O(4) bond distance (2.170(4)) for complex **1**. All the bond lengths and angles are comparable to similar structures [20–22,27,28].

On the other hand in complex **2**, the coordination sphere around the Cu atom consists of three nitrogen atoms from btmpp ligand and two nitrite ions. For a pentacoordinated metal center, the distortion of the coordination environment from a trigonal bipyramidal to a square pyramidal can be evaluated by the trigonality index, τ defined as $\tau = (\alpha - \beta)/60$, where α and β are the two largest coordination angles around the central atom. When $\tau = 0$, the coordination is assumed to be an ideal square pyramid; for

Table 4
Hydrogen bond geometry (Å, °) of compounds **1** and **2**.

	D–H	H···A	D···A	D–H···A	Symmetry	
D–H···A[*]						
1	C(11)–H(12)···O(1)	0.93	2.55	3.432	153	$x, 1/2 - y, -1/2 + z$
2	C(5)–H(3)···O(4)	0.93	2.47	3.197	135	$-x, 1 - y, -z$
	C(7)–H(5)···O(1)	0.96	2.48	3.278	141	$1 - x, 1 - y, -z$
C–H···π						
2	C(7)–H(4)···R3	0.95	2.69	3.567	151	$1 - x, 1 - y, -z$

[*] D: Donor, A: Acceptor, [R1: N(1)–N(2)–C(10)–C(8)–C(6) and R2: N(3)–C(1)–C(2)–C(3)–C(4)–C(5) for **1**], [R3: N(1)–N(2)–C(10)–C(8)–C(6) and R4: N(3)–C(3)–C(2)–C(1)–C(5)–C(4) for **2**].

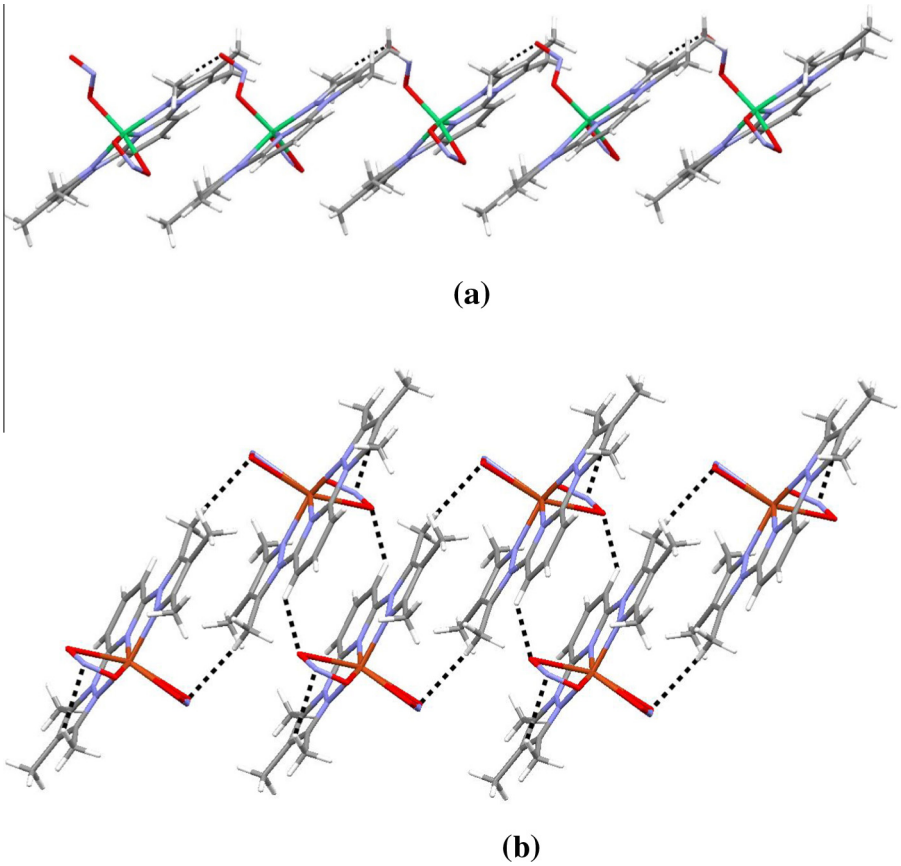

Fig. 3. (a) C–H···O hydrogen bonded structure of **1**. (b) C–H···O hydrogen bonded structure of **2**.

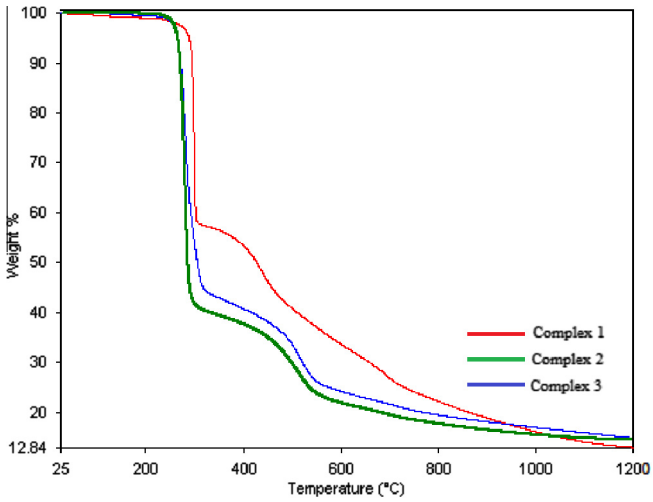

Fig. 4. TG curves of complexes **1**, **2** and **3**.

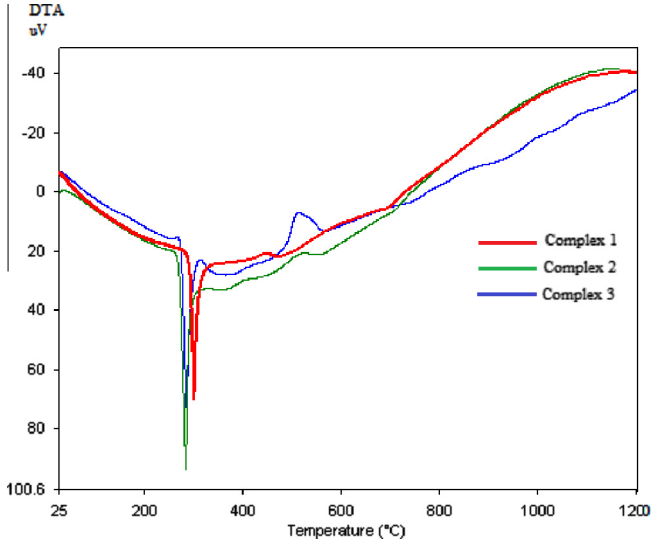

Fig. 5. DTA curves of complexes **1**, **2** and **3**.

an ideal trigonal bipyramid $\tau = 1$ [29]. In our case, the structural distortion indexes of **2** were found $\tau_{Cu1} = 0.083$, indicating that Cu atom adopted a distorted square-pyramidal geometry (Fig. 2). In the coordination network, the Cu–N bond lengths ranged from 1.971(4) to 2.033 (4) Å and Cu–O bond lengths were 2.005(6) and 2.190(2) Å, respectively (Table 3). These observed geometrical features of copper center in **2** are quite comparable to those of the similar complexes reported in the literature [30,31].

C–H···O weak intermolecular interaction connects the molecules in the structure of **1** and **2** which form to 1D chains (Table 4, Fig. 3). Besides that $\pi\ldots\pi$ interactions between the rings (R1...R2^{i} = 3.9066 Å, i = $1-x, 1-y, -z$) for **1** (R3...R4^{ii} = 3.6947 Å, ii = $-x, 1-y, -z$) for **2** were also observed.

3.4. Thermal analysis

To examine the thermal stabilities of the compounds **1**, **2** and **3**, thermogravimetric and differential thermal (TG/DTA) analyses were carried out in nitrogen atmosphere at a heating rate of 20 °C/min from ambient temperature to 1200 °C. TG and DTA curves of complexes are shown in Figs. 4 and 5, respectively. TG/DTA curves indicated that **1** was stable at 190 °C, decomposition of two nitrite and one btmpp ligand was seen in the temperature range of 190–1100 °C (weight loss: calculated, 86.8%; observed, 87.0%) with an exothermic peak at 301 °C. Compound **2** showed thermal stability up to 223 °C and decomposition of two nitrite and one btmpp ligand occured at 223–1200 °C (weight loss: calculated, 85.9%; observed, 85.2%) with an exothermic peak at 283 °C. TG curve of complex **3** showed that the complex was stable up to 233 °C and above this temperature, decomposition of two nitrite and one btmpp ligand started and showed certain weight loss about 85.2% (calculated, 86.8%) in the range of 233–1200 °C. In the DTA curve, there is an exothermic peak at 285 °C for this event. Moreover, the thermogravimetric analyses revealed that all three complexes similarly decomposed to explosive materials.

3.5. DNA cleavage activity of the complexes

In order to investigate the nuclease activity of complexes **1**–**3** and btmpp ligand, agarose gel electrophoresis was carried out following the incubation of these with pET21a plasmid DNA (Novagen, USA). The DNA cleavage behavior of complexes was analyzed by monitoring the conversion of the supercoiled DNA form (Form I) to the nicked (Form II) and linear forms (Form III). The gel picture displaying the DNA molecules is shown in Fig. 6.

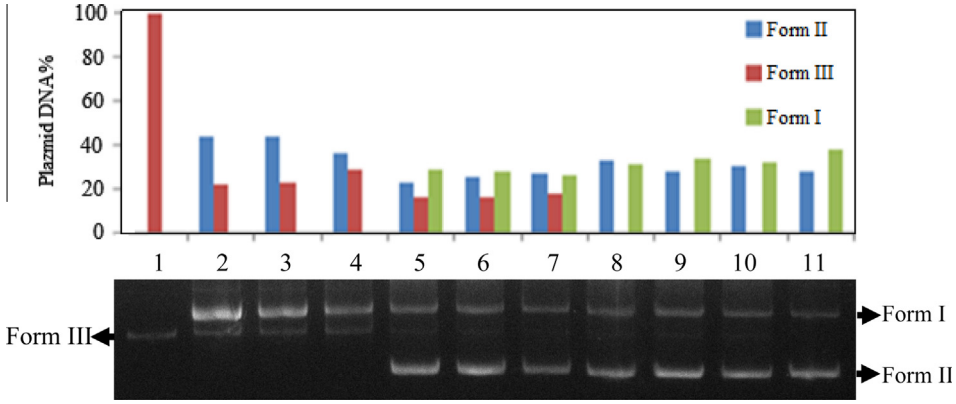

Fig. 6. Electrophoretic mobility assay of pET21a plasmid DNA treated with complexes **1**–**3**. (Lane 1: *Eco*RI digested and linearized pET21a plasmid DNA only, lanes 2–4: DNA + complex **2**, lanes 5–7: DNA + complex **1**, lanes 8–10: DNA + complex **3**, with increasing concentrations of 200, 500 and 1000 μM, respectively. Lane 11, free btmpp ligand). Above the gel is shown a graphic with the plasmid DNA forms' quantification percentages.

It is well known that circular plasmid DNA migrates faster than that of its linear form in electrophoresis due to closed circular conformations. If one strand of DNA is nicked, the supercoil will relax and a slower moving conformation will be produced. If both strands are cleaved, on the other hand, a linear conformation will be generated and it will migrate between Form I and II [32]. Complexes **1** and **2** effectively cleave double stranded DNA even in the absence of any additional external agents and cleavage efficiency of complexes remarkably increases with higher concentrations. Furthermore, the linearization of pET21a plasmid DNA occurs only in complex **1** and **2**, and not with complex **3**. In contrast to the others, complete conversion of supercoiled form both into the nicked and to the linear form was observed with complex **2**.

4. Conclusions

Tridentate NNN type ligand (btmpp) and its nitrito complexes with Ni(II), Cu(II) and Co(II) (**1**–**3**) were synthesized and characterized by spectroscopic and thermal methods. The crystal structure of complexes **1** and **2** has been determined by single crystal diffraction. DNA interaction of compounds was studied by agarose gel electrophoresis method. Electrophoretic experiments support that all of the complexes make conformational changes on plasmid DNA even in the absence of any additional external agents by exerting single strand cleavage and thereby converting supercoiled form to nicked form. Complex **2** more effectively cleaves plasmid DNA and completely converts the supercoiled form to nicked and linear forms.

Acknowledgements

The financial supports of the Scientific and Technical Research Council of Turkey (TUBITAK-TBAG (108T622)) and Balıkesir University are gratefully acknowledged.

Appendix A. Supplementary data

CCDC 743351 and 746794 contain the supplementary crystallographic data for **1** and **2** in this paper. These data can be obtained free of charge from The Cambridge Crystallographic Data Centre via www.ccdc.cam.ac.uk/data_request/cif. Supplementary data associated with this article can be found, in the online version, at http://dx.doi.org/10.1016/j.ica.2014.12.035.

References

[1] H. Sigel, R.B. Martin, Chem. Rev. 82 (1982) 385.
[2] J.W. Peters, M.H.B. Stowell, S.M. Soltis, M.G. Finnegan, M.K. Johnson, D.C. Rees, Biochemistry 36 (1997) 1181.
[3] D.S. Martin, P.K. Mascharak, Chem. Soc. Rev. 29 (2000) 69.
[4] S. Hazra, S. Naskar, D. Mishra, S.I. Gorelsky, H.M. Figgie, W.S. Sheldrick, S.K. Chattopadhyay, Dalton Trans. 37 (2007) 4143.
[5] J. Zhang, Q. Liu, C. Duan, Y. Shao, J. Ding, Z. Miado, X.-Z. You, Z. Guo, J. Chem. Soc., Dalton Trans. 4 (2002) 591.
[6] A.K. Patra, J.M. Rowland, D.S. Marlin, E. Bill, M.M. Olmstead, P.K. Mascharak, Inorg. Chem. 42 (2003) 6812.
[7] Verasuntharam M. Manikandavathavan, Varatharaj Rajapandian, Allen J. Freddy, Thomas Weyhermüller, Venkatesan Subramanian, Eur. J. Med. Chem. 57 (2012) 449.
[8] P.R. Reddy, A. Shilpa, Chem. Biodivers. 8 (2011) 1245.
[9] Li-Na Zhu, De-Ming Kong, Xiao-Zeng Li, Guang-Yu Wang, Jiao Wang, Ya-Wei Jin, Polyhedron 29 (2010) 574.
[10] Orde Q. Munro, W. Roberts Scheidt, Inorg. Chem. 37 (1998) 2308.
[11] D.M.L. Goodgame, M.A. Hıtchman, Inorg. Chem. 4 (5) (1965) 721.
[12] L. El-Sayed, R.O. Ragsdale, Inorg. Chem. 6 (9) (1967) 1644.
[13] S.A. Patil, S.N. Unki, A.D. Kulkarni, V.H. Naik, P.S. Badami, J. Mol. Struct. 985 (2011) 330.
[14] A. Colak, U. Terzi, M. Col, S.A. Karaoglu, S. Karabocek, A. Kucukgudumlu, F.A. Ayaz, Eur. J. Med. Chem. 45 (2010) 5169.
[15] C. Hopa, H. Yildirim, H. Kara, R. Kurtaran, M. Alkan, Spectrochim. Acta, Part A 121 (2014) 282.
[16] C. Hopa, M. Alkan, C. Kazak, N.B. Arslan, R. Kurtaran, Transition Met. Chem. 34 (2009) 403.
[17] SIR92: A. Altomare, G. Cascarano, C. Giacovazzo, A. Guagliardi, M. Burla, G. Polidori, M.J. Camalli, Appl. Cryst. 27 (1994) 435.
[18] P.T. Beurskens, G. Admiraal, G. Beurskens, W.P. Bosman, R. de Gelder, R. Israel, J.M.M Smits, The DIRDIF-99 program system, Technical Report of the Crystallography Laboratory, University of Nijmegen, Netherlands, 1999.
[19] CrystalStructure 3.5.1: Crystal Structure Analysis Package, Rigaku and Rigaku/MSC (2000–2003), 9009 New Trails Dr., The Woodlands, TX 77381, USA.
[20] D.J. Watkin, C.K. Prout, J.R. Carruthers, P.W. Betteridge, CRYSTALS Issue 10: Chemical Crystallography Laboratory, Oxford, UK, 1996.
[21] R.E. Weston, T.F. Brodasky, J. Chem. Phys. 27 (1957) 683.
[22] K. Nakamato, 1st edition., The Infrared Spectra of inorganic and complex molecules, J. Wiley and Sons Inc., 1982.
[23] L. El-Sayed, R.O. Ragsdale, Inorg. Chem. 6 (9) (1967) 1640.
[24] D.M.L. Goodgame, M.A. Hitchman, Inorg. Chem. 3 (10) (1964) 1389.
[25] K. Nakamoto, J. Fujita, H. Murata, J. Am. Chem. Soc. 80 (18) (1958) 4817.
[26] C.A. Bessel, R.F. See, D.L. Jameson, M.R. Churchill, K.J. Takeuchi, J. Chem. Soc., Dalton Trans. (1992) 3223.
[27] N.F. Curtis, H.K.J. Powell, H. Puschmann, C.E.F. Rickard, J.M. Waters, Inorg. Chim. Acta 355 (2003) 25.
[28] J.C. Byun, W.H. Lee, C.H. Han, Inorg. Chem. Commun. 9 (2006) 563.
[29] A.W. Addison, T.N. Rao, J. Reedijk, J. Van Rijn, G.C. Verschoor, J. Chem. Soc., Dalton Trans. 7 (1984) 1349.
[30] B. Sarkar, S. Konar, C.J. Gomez-Garcia, A. Ghosh, Inorg. Chem. 47 (24) (2008) 11611.
[31] C.J. Simmons, A. Clearfield, W. Fitzgerald, S. Tyagi, B.J. Hathaway, Inorg. Chem. 22 (17) (1983) 2463.
[32] P.R. Reddy, P. Manjula, Chem. Biodivers. 4 (2007) 468.